DOI: 10.1534/genetics.107.072090

Suppression of the *Schizosaccharomyces pombe cut12.1* Cell-Cycle Defect by Mutations in *cdc25* and Genes Involved in Transcriptional and Translational Control

Victor A. Tallada, Alan J. Bridge,[1] Patrick A. Emery[2] and Iain M. Hagan[3]

CRUK Cell Division Group, Paterson Institute for Cancer Research, University of Manchester, Manchester M20 4BX, United Kingdom

Manuscript received November 9, 2006
Accepted for publication February 22, 2007

ABSTRACT

Cdc25 phosphatase primes entry to mitosis by removing the inhibitory phosphate that is transferred to mitosis promoting factor (MPF) by Wee1 related kinases. A positive feedback loop then boosts Cdc25 and represses Wee1 activities to drive full-scale MPF activation and commitment to mitosis. Dominant mutations in the *Schizosaccharomyces pombe* spindle pole body (SPB) component Cut12 enable *cdc25.22* mutants to overcome a G2 arrest at 36° and enter mitosis. The recessive temperature-sensitive *cut12.1* mutation results in the formation of monopolar spindles in which the spindle pole marker Sad1 is enriched on the nonfunctional SPB at 36°. We identified mutations at five loci that suppressed the lethality of the recessive *cut12.1* mutation at 36° and conferred lethality at 20°. Three of the five mutations led to the formation of monopolar spindles at restrictive temperatures, affected cell size at commitment to mitosis, and generated multiple Sad1 foci at nuclear periphery. The five loci, *tfb2.rt1*, *tfb5.rt5*, *pla1.rt3*, *rpl4301.rt4*, and *rot2.1*, and multicopy suppressors, including $tfb1^+$ and $dbp10^+$, are involved in transcription, translation, or RNA processing, prompting us to establish that elevating Cdc25 levels with the dominant *cdc25.d1* allele, suppressed *cut12.1*. Thus, *rot* mutants provide a further link between protein production and cell-cycle progression.

GENETIC analysis of cell-cycle control in fission yeast and biochemical approaches in Xenopus revealed that commitment to mitosis is controlled by the activity of a conserved protein kinase complex called mitosis promoting factor (MPF) (Nurse 1990). MPF is composed of a catalytic subunit, Cdc2 (known as Cdk1 in several systems), and a regulatory subunit, cyclin B, that is destroyed when cells enter anaphase (Evans *et al.* 1983). Cdc2 is activated only when the criteria for entrance to mitosis have been fulfilled. In fission yeast these criteria include the attainment of a critical cell volume and the provision of an appropriate nutrient supply to ensure the completion of division (Mitchison 2003). MPF is restrained in an inactive state as a result of inhibitory phosphorylation by Wee1-related kinases until such criteria are fulfilled (Russell and Nurse 1987a; Gould and Nurse 1989; Featherstone and Russell 1991; Parker and Piwnicaworms 1992; McGowan and Russell 1993). This phosphate is then removed at the appropriate time by Cdc25 phosphatase to promote entrance into mitosis (Russell and Nurse 1986). Thus the timing of entrance into mitosis is governed by the balance of Wee1 and Cdc25 activities (Fantes 1983; Nurse 1990).

The activation of a priming level of MPF promotes a positive feedback loop that boosts the activity of Cdc25 and inhibits the activity of Wee1-related kinases (Hoffmann *et al.* 1993). Studies of MPF activation in Xenopus extracts indicated that, while MPF itself comprised an important part of this positive feedback loop, Cdc25 could still be activated in MPF primed extracts from which all Cdc2 and the related Cdk2 kinase had been depleted and that mutation of MPF consensus phosphorylation sites on Cdc25 did not block activation (Izumi and Maller 1993, 1995). The search for the feedback loop, Cdc25 activating, kinase identified Xenopus polo kinase (Kumagai and Dunphy 1996). Subsequent work consolidated the view that polo kinase constitutes a critical part of the loop in Xenopus extracts (Abrieu *et al.* 1998; Karaiskou *et al.* 1999, 2004). Furthermore, phosphorylation of cyclin B by polo kinase is one of the earliest aspects of MPF activation noted in human cells to date (Jackman *et al.* 2003) and injection of antibodies against polo kinase blocks entrance to mitosis in nontransformed human cell lines (Lane and Nigg 1996). Less is known of Wee1's role in feedback loop activation; however, it is heavily phosphorylated

[1]*Present address:* Swiss Institute of Bioinformatics (SIB), CH-1211 Geneva 4, Switzerland.

[2]*Present address:* Matrix Science, London W1H 1PP, United Kingdom.

[3]*Corresponding author:* CRUK Cell Division Group, Paterson Institute for Cancer Research, Wilmslow Rd., Manchester M20 4BX, United Kingdom. E-mail: ihagan@picr.man.ac.uk

upon mitotic commitment in a range of systems (Tang *et al.* 1993; Mueller *et al.* 1995; Watanabe *et al.* 2004) and budding yeast Wee1, Swe1, has been proposed to interact with and be inhibited by the polo kinase Cdc5 (Bartholomew *et al.* 2001; Sakchaisri *et al.* 2004). Recent data suggest that Greatwall kinase works alongside polo as part of the positive feedback loop in Xenopus extracts (Yu *et al.* 2006).

In *S. pombe*, the activation of bulk Cdc25 activity requires prior activation of MPF, indicating that it also employs a positive feedback to promote mitosis (Kovelman and Russell 1996). A screen for extragenic suppressors of the conditional *cdc25.22* mutation identified three dominant mutations in the *stf1*$^+$ gene (suppressor of 25) that enabled cells from which *cdc25*$^+$ had been deleted to proliferate (Hudson *et al.* 1990, 1991). The same gene was identified in a screen for mutants that increased ploidy after a generation at 36° (Bridge *et al.* 1998). As the mutant identified in this screen exhibited the "cut" phenotype (Hirano *et al.* 1986), it was called *cut12*$^+$. Because the conditional lethal *cut12.1* mutation was a recessive mutation and *stf1.1* dominant, the gene is referred to as *cut12*$^+$ and the ***stf1.1*** mutation as *cut12.**s11***.

cut12$^+$ encodes an essential component of the spindle pole body (SPB) (Bridge *et al.* 1998). In *cut12.1* mutants one of the two SPBs fails to nucleate microtubules and the SPB-associated protein Sad1 (Hagan and Yanagida 1995) becomes asymmetric, associating primarily with the inactive SPB. Deletion of the *cut12*$^+$ gene also blocks spindle formation, but in this case Sad1 shows equal affinity for either SPB (Bridge *et al.* 1998). In contrast spindle formation and function are unaffected in the *cdc25.22*-suppressing *cut12.s11* allele. Fission yeast polo kinase Plo1 normally associates with the mitotic but not interphase SPBs; however; in *cut12.s11* cells Plo1 is prematurely recruited to interphase SPBs (Mulvihill *et al.* 1999). Furthermore the *cut12.s11* mutation boosts Plo1 kinase activity over wild-type levels, whereas *cut12.1* blocks the mitotic activation of Plo1 (MacIver *et al.* 2003). Genetic analyses support a functional link between Cut12 and Plo1 activity because the ability of *cut12.s11* to suppress *cdc25.22* requires a fully functional Plo1 kinase and activation of Plo1 independently of any change in Cut12 status mimics *cut12.s11* in suppressing *cdc25.22* (MacIver *et al.* 2003). Because inactivation of Wee1 overcomes the requirement for Cdc25 (Fantes 1979) and *Schizosaccharomyces pombe* utilizes a positive feedback loop to promote mitosis (Kovelman and Russell 1996), we proposed that *cut12.s11* suppresses defective Cdc25 function by inappropriately promoting Plo1 activity to drive the feedback loop to suppress Wee1 activity. Implicit in this model is a role for Cut12 in the normal controls that regulate mitotic commitment (MacIver *et al.* 2003).

The ability of the *cut12.s11* allele to promote mitosis in *cdc25.22* cells and the premature recruitment of Plo1 to the SPB both depend upon the activities of the fission yeast NIMA-related kinase, Fin1, and the p38 equivalent stress response pathway (SRP) kinase Spc1/Sty1 (Grallert and Hagan 2002; Petersen and Hagan 2005). Because the amplitude of SRP signaling is greater in minimal than in rich medium (Shiozaki and Russell 1995), Cut12, Plo1, and the SRP coordinate cell division with the nutrient status of the immediate environment.

A further level of control over the timing of commitment to mitosis in fission yeast is provided by modulation of the level of the mitotic inducers. Both Cdc25 and Cdc13/cyclin B accumulate during interphase to peak in mitosis (Booher and Beach 1988; Creanor and Mitchison 1994). Furthermore, both Cdc25 and the two B-type cyclins, Cdc13 and Cig2, are subject to strict translational control (Daga and Jimenez 1999; Grallert *et al.* 2000). A sudden reduction in the competence to translate proteins leads to a precipitous drop in cyclin B levels leading to a rapid block of division upon nutrient limitation (Grallert *et al.* 2000). Similar mechanisms may be employed during checkpoint responses to DNA damage as a DEAD box helicase that has been associated with translational control was identified by a number of groups in a screen of elements that cooperated with Cdc25 to block division when DNA integrity is compromised (Forbes *et al.* 1998; Grallert *et al.* 2000) and in a screen for multicopy suppressors of a cold-sensitive, loss-of-function mutant of *cdc2* (Liu *et al.* 2002).

We describe mutations in five loci that both suppress *cut12.1* lethality at 36° and confer a cold-sensitive growth defect in their own right. These loci are involved in transcription/translation control. The intimate link between Cdc25 and Cut12 and translational control of Cdc25 (Daga and Jimenez 1999) led us to establish that mutations that elevate Cdc25 levels by removing pseudo-ORFs from the *cdc25* 5′-UTR (Daga and Jimenez 1999) suppresses *cut12.1*.

MATERIALS AND METHODS

Strains, cell culture, and molecular biology: Strains are listed in Table 1. Standard fission yeast and molecular biology approaches were used throughout (Moreno *et al.* 1991). For spot tests, cells were grown to midlog phase and serial fivefold dilutions were plated on solid medium. *rotx*-suppressing plasmids were cloned from a genomic library (Barbet *et al.* 1992). To generate the *cdc25.d1::leu1* strain, the *Pst*I–*Sac*I fragment from the plasmid pRep3x:cdc25-d1 (Daga and Jimenez 1999) was cloned into pJK148 integrative plasmid (Keeney and Boeke 1994) to generate pJKcdc25-d1. The new plasmid was linearized into the *leu1*$^+$ marker at the *Nru*I site and transformed into *leu1–32, ura4–d18* strain. Leu+ colonies were selected and checked by PCR and crossing to a leu1::ura4+ strain (0% leu+ ura+) for integration into *leu1* locus (strain IH4625).

Cell biology: Cells were processed for Western blotting with AP9.2 (anti-Sad1), anti-Cut12, anti-Cdc2 (PN24), or 9E.10 anti-myc epitope monoclonal antibody (Evan *et al.* 1985; Simanis and Nurse 1986; Hagan and Yanagida 1995; Bridge *et al.* 1998) according to MacIver *et al.* (2003). Standard fluorescence procedures that used AP9.2 (anti-Sad1) and TAT1 (anti-α

TABLE 1

List of strains

Strain	Genotype	Origin
IH 163	*972 h⁻*	Lab stock
IH 365	*leu1.32 ura4.d18 h⁻*	Lab stock
IH 366	*leu1.32 ura4.d18 his2 h⁺*	Lab stock
IH 3589	*tfb2.rt1 leu1.32 ura4.d18 h⁻*	This study
IH 3968	*tfb2.rt1 ura4.d18 leu1.32 ade6-M210 h⁺*	This study
IH 3979	*tfb2.rt1/tfb2⁺ mei1⁺/mei1.102 ade6.M210/ade6.M216*	This study
IH 693	*tfb2.rt1 cut12.1 ura4.d18 leu1.32 h⁻*	This study
IH 4050	*tfb2.rt1 ura4.d18 leu1.32 cdc25⁺* pRep3X*cdc25.d1 h⁺*	This study
IH 4051	*tfb2.rt1ura4.d18 leu1.32* pREP3X*ded1⁺ h⁺*	This study
IH 3735	*rot2.1 ura4.d18 leu1.32 h⁺*	This study
IH 3969	*rot2.1 leu1.32 ade6-M210 h⁻*	This study
IH 3980	*rot2.1/rot2⁺ mei1⁺/mei1.102 ade6.M210/ade6.M216*	This study
IH 3536	*rot2.1 cut12.1 ura4.d18 leu1.32 h⁺*	This study
IH 2024	*pla1.rt3 cut12.1 his2 leu1.32 ura4.d18 h⁺*	This study
IH 3970	*pla1.rt3 leu1.32 ade6-M210 h⁻*	This study
IH 3981	*pla1.rt3/pla1⁺ mei1⁺/mei1.102 ade6.M210/ade6.M216*	This study
IH 4060	*pla1.rt3 ura4.d18 leu1.32 cdc25⁺* pRep3X*cdc25.d1 h⁻*	This study
IH 4061	*pla1.rt3 ura4.d18 leu1.32* pRep3X*ded1⁺ h⁻*	This study
IH 3537	*rpl4301.rt4 cut12.1 ura4.d18 leu1.32 h⁺*	This study
IH 3290	*rpl4301.rt4 ura4.d18 leu1.32 h⁻*	This study
IH 3291	*rpl4301.rt4 ura4.d18 leu1.32 h⁺*	This study
IH 3982	*rpl4301.rt4/rpl4301⁺ mei1⁺/mei1.102 ade6.M210/ade6.M216*	This study
IH 3292	*tfb5.rt5 ura4.d18 leu1.32 h⁻*	This study
IH 3293	*tfb5.rt5 ura4.d18 leu1.32 his2 h⁺*	This study
IH 3538	*tfb5.rt5 cut12.1 ura4.d18 leu1.32 h⁺*	This study
IH 4035	*tfb5.rt5/rot5⁺ mei1⁺/mei1.102 ade6.M210/ade6.M216*	This study
IH 3604	*tfb5.rt5 cdc25.22 ura4.d18 leu1.32 his2 h⁻*	This study
IH 4070	*tfb5.rt5 ura4.d18 leu1.32 cdc25⁺* pRep3X*cdc25.d1 h⁻*	This study
IH 4071	*tfb5.rt5 ura4.d18 leu1.32* pRep3*Xded1⁺ h⁻*	This study
IH 596	*cut12.1 leu1.32 ura4.d18 h⁻*	Bridge *et al.* (1998)
IH 661	*cut12.1 ade6.704 ura4.d18 leu1.32 his2 h⁺*	Bridge *et al.* (1998)
IH 3496	*ded1-61 leu1.32 h⁻*	Grallert *et al.* (2000)
IH 3497	*ded1-78 leu1.32 h⁻*	Grallert *et al.* (2000)
IH 3541	*ded1-1D5 ura4.d18 leu1.32 h⁺*	Grallert *et al.* (2000)
IH 5464	*cut12.1 ded1-1D5 h⁻*	This study
IH 5466	*cut12.1 ded1-78 h⁻*	This study
IH 4626	*leu1::cdc25.d1 cdc25⁺cut12.1 h⁻*	This study
IH 4625	*leu1::cdc25.d1 cdc25⁺ h⁺*	This study
IH 634	*cdc25.22 ura4.d18 leu1.32 his2 h⁺*	Lab stock
IH 565	*cdc25.22 ura4.d18 leu1.32 h⁻*	Lab stock
IH 333	*gtb1⁺:LEU2⁺ leu1.32 h⁻*	This study
IH3029	*h⁺ cdc25:12myc:ura4⁺ ura4.D18 leu1.32*	Lopez-Girona *et al.* (1999)
IH4461	*h⁻ tfb2.rt1 cdc25:12myc:ura4⁺ ura4.D18 leu1.32*	This study
IH4394	*h⁻ rot2.1 cdc25:12myc:ura4⁺ ura4.D18 leu1.32*	This study
IH4395	*h⁻ pla1.rt3 cdc25:12myc:ura4⁺ ura4.D18 leu1.32*	This study
IH4396	*h⁻ rpl4301.rt4 cdc25:12myc:ura4⁺ ura4.D18 leu1.32*	This study
IH3598	*h⁺ tfb5.rt5 cdc25:12myc:ura4⁺ ura4.D18 leu1.32*	This study

tubulin) antibodies were as described previously (Woods *et al.* 1989; Hagan and Yanagida 1995). Images were obtained using either a Deltavision Spectris system or an inverted Zeiss axioplan II with a coolsnap camera (Photometrics) driven by the Metamorph (Universal Imaging). Metamorph was used to measure cell lengths. For Figure 4, E and D, and Figure 6C a series of 10–12 × 0.3-μm slices of a single field was captured on the deltavision imaging platform to generate a series of images in the *Z* axis that was compressed to give the maximal projections shown in Figure 4, E and D, and Figure 6C.

RESULTS

Isolation of revertants of cut twelve mutants: To identify genes that displayed genetic interactions with *cut12⁺*, 1000 spontaneous mutants that enabled *cut12.1* cells to form colonies at 36° were isolated and streaked at 20° to identify 45 strains that were unable to grow at the lower temperature. Five mutants displayed a strong cold-sensitive phenotype when crossed away from *cut12.1*

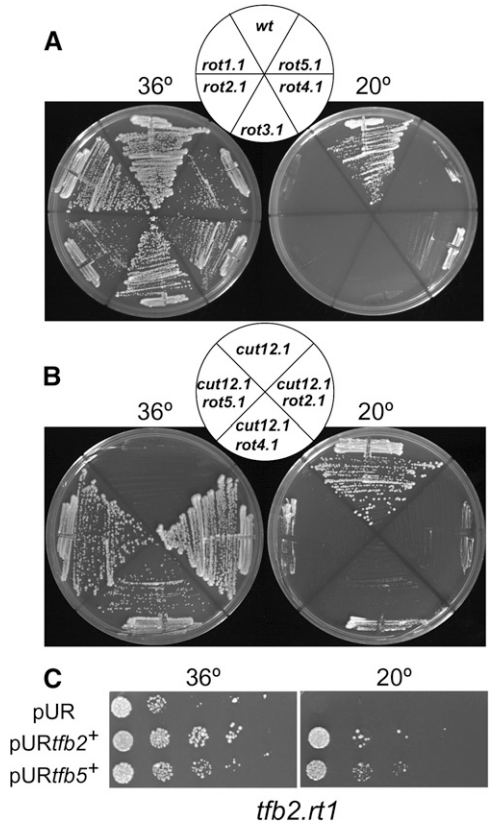

FIGURE 1.—Cold-sensitive *rot*⁻ mutants suppress the *cut12.1* deficiency at 36°. The indicated strains were streaked (A and B) or spotted as serial dilutions (C) onto rich YES medium at the indicated temperatures.

into a *cut12*⁺ background (Figure1A). After two further backcrosses, linkage analysis established that the mutants fell into five separate complementation groups, *rot1–5* (*r*evertant *o*f *t*welve). The mutations were reintroduced into the *cut12.1* background to confirm that the cold-sensitive mutation did indeed compensate for the *cut12.1* defect (Figure 1B). Generation of stable *cut12.1/cut12.1 ade6.M210/ade6.M216 mat1.102/h- rotx.1/rotx*⁺ heterozygous diploids established that all alleles selected for further characterization were recessive with respect to both suppression of *cut12.1* and cold sensitivity (data not shown).

Cloning of *rot* genes: With the exception of *rot5*⁺, all *rot* genes were cloned by complementation of the cold-sensitive growth defect of *rot* alleles. As attempts to clone *rot5*⁺ by complementation of *rot5.1* isolated the same DEAD box helicase gene *dbp10*⁺ as a multicopy suppressor in 98 separate transformants, we employed a strategy to generate a genomic library that lacked this gene. The pURB2 library (BARBET *et al.* 1992) was amplified in *Escherichia coli*, to generate around 5000 colonies on each of 44 plates. DNA was prepared separately from each plate and PCR identified 27 pools that contained the *dbp10*⁺ ORF. The remaining 17 pools were combined to create a library with a complexity of 85,000 [the complexity of the original library was 105,000 clones (BARBET *et al.* 1992)]. Transformation of this selected library into *rot5.1* cells generated two colonies at restrictive temperature that contained the ORF *SPBC32F12.15*. Sequences adjacent to the *gtb1*⁺/*tug1*⁺ locus that lies 16.7 kb from ORF *SPBC32F12.15* were used to integrate the *LEU2*⁺ gene adjacent to the *gtb1*⁺/*tug1*⁺ locus and subsequent crossing to *rot5.1* established tight linkage (8.6 cM). Crossing *rot5.1* to this *LEU2+* marker gave no recombinants in over 200 random spores Sequencing the *SPBC32F12.15* ORF identified a substitution of proline for alanine in the the fourth codon of the protein indicating that *SPBC32F12.15* is indeed *rot5*⁺.

***rot*⁺ genes encode molecules that modulate protein production:** The *rot*⁺ genes and corresponding multicopy suppressors were predicted to encode molecules implicated in the control of protein production at the level of transcription, translation, or RNA processing (Table 2). The *rot1/tfb2*⁺ and *rot5*⁺/*tfb5*⁺ genes and a suppressor of *rot4.1* (*tfb1*⁺) encoded conserved components of the TFIIH complex that plays a critical role in promoting cell-cycle-dependent transcription of a subset of *S. pombe* genes (LEE *et al.* 2005). This predicted functional relationship was supported by genetic interactions as *rot1.1* (hereafter referred to as *tfb2.rt1*) displayed synthetic lethality with *rot5.1* (hereafter referred to as *tfb5.rt5*) and the introduction of a multicopy plasmid harboring the *tfb5*⁺ gene was able to complement the cold sensitivity of *tfb2.rt1* (Figure 1C). *rot3*⁺/*pla1*⁺ encodes the essential nuclear poly(A) polymerase (OHNACKER *et al.* 1996; DING *et al.* 2000; STEVENSON and NORBURY 2006). *rot4*⁺ encoded the Rpl4301 component of the 60S ribosomal complex. A second *rpl4302*⁺ gene that differs by just four amino acids was isolated as a multicopy suppressor of *rot4.1* (hereafter referred to as *rpl4301.rt4*). The *rot2*⁺ gene and multicopy suppressors of *rot2.1* and *tfb5.rt5* encode DEAD/DEAH box helicases.

***rot* mutations alter size at division and spindle pole function:** Because *cut12* alleles exhibit cell-cycle and spindle formation phenotypes, the microtubule cytoskeleton and length at division of *rot* mutants was assessed. With the exception of the *rpl4301.rt4* mutant that showed no deviation from wild type after two generations at restrictive temperature, all *rot* mutations altered the number of cells in mitosis at any one time, the size at which cells committed to mitosis and increased the size and number of Sad1 foci at the nuclear periphery and the appearance of Sad1 foci at some distance from the chromatin. Importantly, three phenocopied *cut12.1* in forming monopolar rather than bipolar spindles (Table 3 and Figures 2–4).

Monopolar spindles were associated with chromosome segregation errors in both TFIIH components identified in the screen; *tfb2.rt1* cells had monopolar spindles at 20°, while *tfb5.rt5* phenocopied the *cut12.1* monopolar phenotype at the semipermissive temperature of 30° but not at the restrictive 20° (Figures 2B, 3B, and 3C; Table 3). At the permissive temperature of 36° *tfb5.rt5* cells exhibited

TABLE 2

Suppressors of *rot* mutants encode transcription and translation factors

Mutant	Gene	Product	Biological function
tfb2.rt1	*tfb2*$^+$	Transcription factor TFIIH complex	Transcription (E)
rot2.1	*rot2*$^+$	DEAD/DEAH box helicase	RNA export (P)
pla1.rt3	*pla1*$^+$	Poly(A) polymerase	RNA poly-adenylation (E)
rpl4301.rt4	*rpl4301*	60S ribosomal protein	Translation (P)
tfb5.rt5	*tfb5*$^+$	Transcription factor TFIIH complex	Transcription (P)

Mutant	aa identity to human homologs (%)	Multicopy suppressors
tfb2.rt1	45	NF
rot2.1	47, 35, 29	DEAD/DEAH box helicase SPBC13G1.10c Pseudo C-terminal DNA helicase SPAC212.06c
pla1.rt3	47, 47, 46	NF
rpl4301. rt4	58	*tfb1*$^+$ (TFIIH complex) *rpl4302*$^+$
tfb5.rt5	25	*dbp10*$^+$ (DEAD/DEAH box helicase)

P, predicted by sequence; E, experimental; NF, not found.

a range of morphogenetic defects including cell bending to generate the *ban*$^-$ phenotype (Figure 3A) (Verde *et al.* 1995).

The proportion of the population of *rot2.1* cells that formed monopolar spindles was also influenced by the culture temperature as 5% of all mitoses at 36° had monopolar spindles whereas 38% have monopolar spindles at 18° (Figure 4, A, C, and D; Table 3). The *rot2.1* mutation had a further impact upon spindle architecture as there was a marked proliferation of Sad1 foci around the periphery nuclei and some dots seen away from the chromatin of *rot2.1* cells at both the restrictive and permissive temperature (Figure 4, A–D, data not shown). This alteration in Sad1 distribution was not always associated with the formation of a monopolar spindle (Figure 4, A and B). Furthermore, the distribution of the core SPB components Cut12 and Sid4 was not affected by the *rot2.1* mutation (Figure 4, E and F, data not shown). Thus the excess Sad1 foci neither acted as spindle poles nor contained all SPB components. The radical changes in Sad1 distribution were not mirrored by a significant enhancement of protein levels (Figure 4G), suggesting that the *rot2.1* mutation affected the recruitment of Sad1 protein to sites on the nuclear envelope. *rot2.1* cells

TABLE 3

***rot* mutants phenotypes**

			Mislocalization of Sad1			
	Length at mitosis (μm)		Interphase		Mitosis	
Mutant	36°	20°	36°	20°	36°	20°
tfb2.rt1	11.7 ± 0.9	15.8 ± 1.6	Yes	No	No	No
rot2.1	11.7 ± 2.6	12.4 ± 3.5	Yes	Yes	Yes	Yes
pla1.rt3	9.3 ± 1.5	11.0 ± 1.5	No	Yes	No	No
rpl4301.rt4	13.4 ± 1.7	14.0 ± 1.1	No	No	No	No
tfb5.rt5	14.0 ± 1.4	17.0 ± 2.3	Yes	Yes	No	Yes
ded1-61	15.0 ± 1.2	17.1 ± 1.5	No	Yes	No	No
wt	13.9 ± 0.96	14.6 ± 1.5	No	No	No	No
	Cells in mitosis (%)		Monopolar spindles (%)		PAAs (%)	
Mutant	36°	20°	36°	20°	36°	20°
tfb2.rt1	6	22	No	10	21	25
rot2.1	8	16	5	38	8	34
pla1.rt3	6	2	No	No	35	15
rpl4301.rt4	8	7	No	No	15	14
tfb5.rt5	7	15	14	30	3	15
wt	8	7	No	No	14	15

PAAs, post-anaphase arrays. $n = 200$.

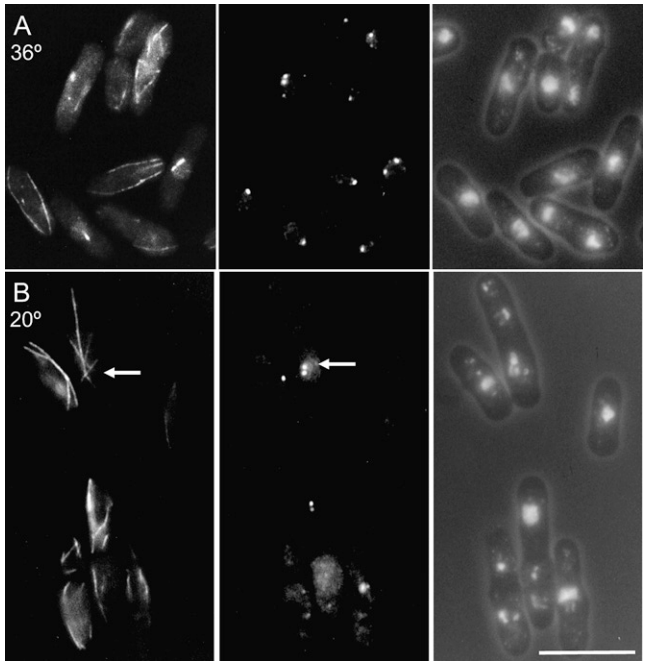

Figure 2.—*tfb2.rt1* mutants form monopolar spindles at the restrictive temperature. *tfb2.rt1*cells were grown to early log phase at 36° (A) before the temperature of the medium was changed to 20° (B). Immediately before and 24 hr after the shift cells were processed for indirect immunofluorescence to reveal the distribution of microtubules (left), Sad1 protein (middle), and the relative location of the chromatin (right). Arrows indicate the two SPBs of a late mitotic spindle in a cell that is just forming a post-anaphase array even though chromosome segregation has not occurred. Bar, 10 μm.

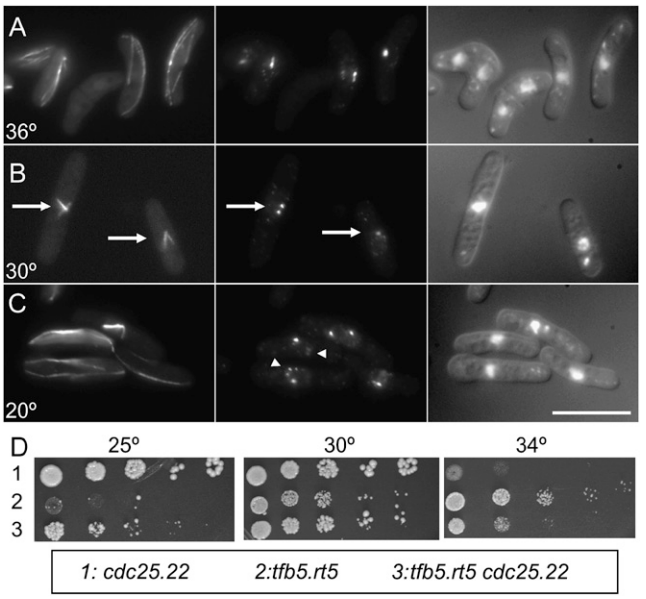

Figure 3.—The *tfb5.rt5* mutation compromises spindle formation at 30°, increases the number of Sad1 foci on interphase nuclei at 20°, and compensates for the *cdc25.22* growth defect at 34°. (A–C) *tfb5.rt5* cells were grown to early log phase at 36° before the temperature of the medium was changed to 30° or 20°. Immediately before (A) and 12 hr after the shift to 30° (B) and 20 hr after the shift to 20° (C) cells were processed for indirect immunofluorescence to reveal the distribution of microtubules (left), Sad1 protein (middle), and the relative location of the chromatin (right). Arrows in B indicate monopolar spindles, while arrowheads in C point to multiple Sad1 foci on an interphase nucleus. We assume that the largest of these foci is the SPB. Bar, 10 μm. (D) Spot tests of serial dilutions show that the *tfb5.rt5 cdc25.22* strain grows more efficiently than either single mutant at 34° or 25°, respectively.

divided at reduced cell size and had alterations in the control of the final stages of cytokinesis because there were fewer cells with two separated nuclei and post-anaphase arrays of microtubules at the permissive temperature (8% *vs.* 15% for wild-type control), yet more at the restrictive (34% *vs.* 14% for wild-type control; Table 3).

pla1.rt3 mutant phenotype resembled that of *rot2.1* except that cells did not form monopolar spindles. Cell length at division was decreased, and there was a proliferation of Sad1 foci without an obvious increase in Sad1 protein levels (Figures 5 and 4G) and an accumulation of cells with post-anaphase microtubule arrays (35% at permissive; Table 3). While the figure of 15% post-anaphase arrays seen at the restrictive is reminiscent of the wild-type value of 14%, the proportion of cells in the preceding phase of the cell cycle (those with mitotic spindles) was radically reduced (2% *vs.* 7%) (Table 3; Figure 5). As a reduction in the numbers of spindles should similarly reduce the number of cells in subsequent stages of the cell cycle, the data suggest that *pla1.rt3* also delays the completion of cell fission at the restrictive temperature.

Similarities between *ded1/sum3*$^-$ and *rot*$^-$ phenotypes: As the current screen established that DEAD box helicases exhibited genetic interactions with a *cdc25.22* suppressor, and the DEAD box helicase Ded1/Sum3 has been linked to Cdc25 and Cdc2 function in mitotic control (Forbes *et al.* 1998; Grallert *et al.* 2000; Liu *et al.* 2002), we assessed the status of the microtubule cytoskeleton in *ded1.61* cells. These cold-sensitive cells were incubated at 18° for 12 hr before processing to reveal the microtubule cytoskeleton and chromatin. The length at which cells entered mitosis increased (Table 3) and multiple Sad1 foci accumulated around the interphase nuclei and away from the chromatin of bent cells in which microtubules curled around cell tips (Figure 6). The increase in the number of Sad1 foci was not accompanied by a radical change in Sad1 levels (Figure 4G). The similarity of these phenotypes to those of the *rot* mutants prompted us to ask whether multicopy levels of *ded1*$^+$ could mimic the DEAD/DEAH box helicases identified in this study in suppressing *cut12.1*; however, it could not. Second we asked whether the incorporation of *ded1.61* alongside *cut12.1* in the same cell mimicked the rot mutants in suppressing the lethality of *cut12.1* at 36°; however, the double mutant was synthetically lethal at both 30° and 36°. A potential overlap between *ded1*$^+$ and *rot* genes was revealed by the inviability of *tfb5.rt5 ded1.61* double mutants at 36° that is normally permissive for either mutant.

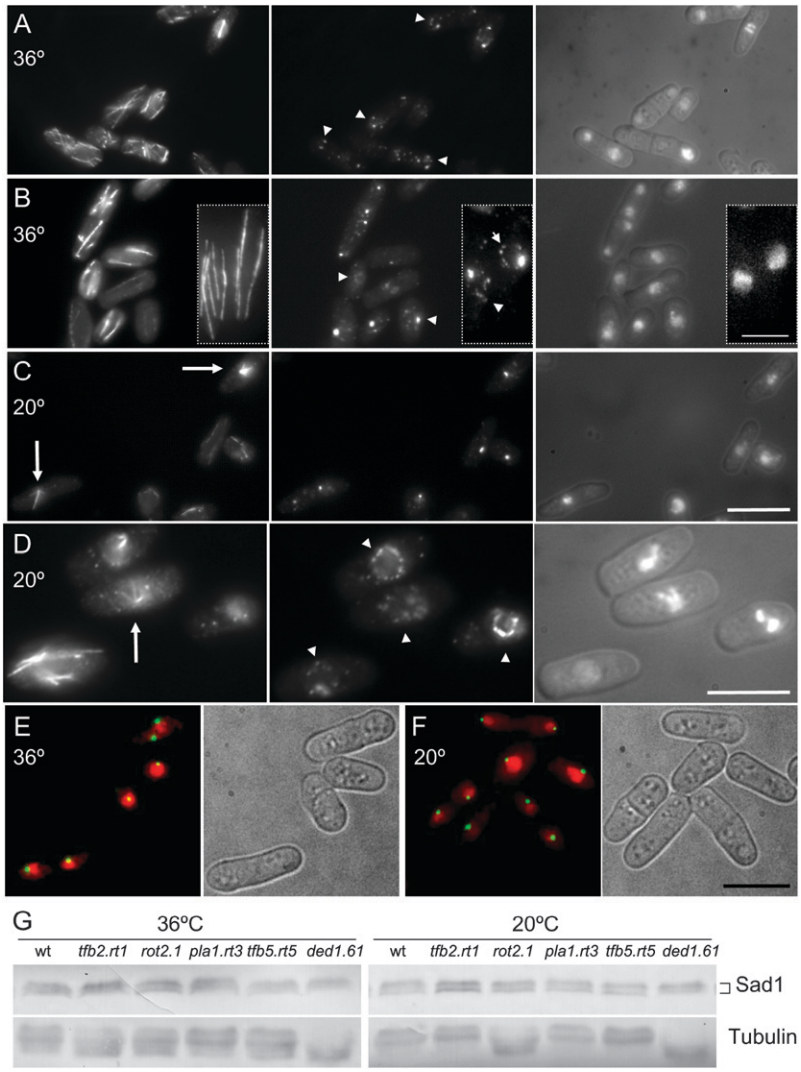

FIGURE 4.—*rot2.1* mutants form monopolar spindles and multiple Sad1 foci around their nuclear periphery. (A–D) *rot2.1* cells were grown to early log phase at 36° before the temperature of the medium was changed to 20°. Immediately before (A and B) and 15 hr after (C and D) the shift cells were processed for indirect immunofluorescence to reveal the distribution of microtubules (left), Sad1 protein (middle), and the relative location of the chromatin (right). Arrowheads in A, B, and D indicate the additional spots of Sad1 staining seen on the nuclear periphery while arrows in C and D identify monopolar spindles. Bars, 10 μm; bar in inset, 5 μm. (E and F) Live cell imaging of *rot2.1 cut12.NEGFP* cells stained with Hoescht 33342 to reveal Cut12 (green) alongside chromatin (red) and brightfield images of cell outlines. While Sad1 forms multiple foci (A–D) the Cut12.GFP signal is still a single discrete dot, indicating that the extra dots of Sad1 seen in *rot2.1* cells do not contain Cut12. Imaging cells expressing Sid4.Tdtom also gave single dots at all temperatures (data not shown). (G) Western blots of cell extracts from the indicated strains probed with either AP9.2 anti-Sad1 antibody (top) or TAT1 anti-tubulin (bottom). The altered migration of the tubulin bands was seen in multiple independent experiments. We have not established the nature of the modification that underlies this change in protein migration.

***cdc25.d1* suppresses *cut12.1*:** One model to account for the identification of molecules that have the potential to modulate the abundance of proteins in a screen for *cut12.1* suppressors is that they altered the levels of molecules related to Cut12 function and so enabled the compromised version of Cut12.1 to perform the essential function executed by the wild-type molecule sufficiently well for the cells to survive. As Cut12 modulates pathways that control entrance to mitosis and both Cdc25 and B-type cyclins are exquisitely sensitive to changes in translational control (DAGA and JIMENEZ 1999; GRALLERT *et al.* 2000), we asked whether elevating the levels of Cdc25 or the major B-type cyclin (FISHER and NURSE 1996), Cdc13, would suppress *cut12.1*.

Cdc13 levels were elevated by inducing the gene on a multicopy plasmid while Cdc25 levels were enhanced by integrating the *cdc25.d1* allele at the *leu1* locus under the control of the *nmt1*$^+$ promoter. The removal of three pseudo-ORFs in the 5′ region of the *cdc25*$^+$ UTR greatly increases the amount of the phosphatase that is produced from the mutant *cdc25.d1* gene (DAGA and JIMENEZ 1999). Increasing *cdc13*$^+$ dosage did not suppress *cut12.1*; however, the introduction of the *cdc25.d1* allele did (Figure 7A). In time lapse microscopy of strains harboring the tubulin–GFP fusion gene *atb2.GFP*, only 4 of 31 *cut12.1* cells formed bipolar mitotic spindles and completed division (Figure 7B), while 29 of 37 *cut12.1 cdc25.d1* mutants successfully completed mitosis (Figure 7C).

A further link between the *cut12* and *cdc25* emerged when we asked whether any of the *rot* genes exhibited a genetic interaction with *cdc25.22* as *tbf5.rt52 cdc25.22* double mutants were healthier at 25° than *rot5.2* and healthier at 34° than *cdc25.22* (Figure 3D).

***rot* mutations reduce the levels of Cdc25 and Cut12:** The finding that alteration of the levels of a key mitotic inducer suppressed the conditional lethality of *cut12.1* prompted us to ask whether this formed the basis of the suppression of *cut12.1* by these mutations. We therefore generated strains that combined the *cdc25.myc* allele (LOPEZ-GIRONA *et al.* 1999) alongside each *rot* mutant and blotted extracts to relate the amount of Cdc25.myc to a standard loading control, Cdc2 (SIMANIS and NURSE 1986) (Figure 8A). The relative levels of Cdc25.myc were reduced below those seen in wild-type cells in all *rot*

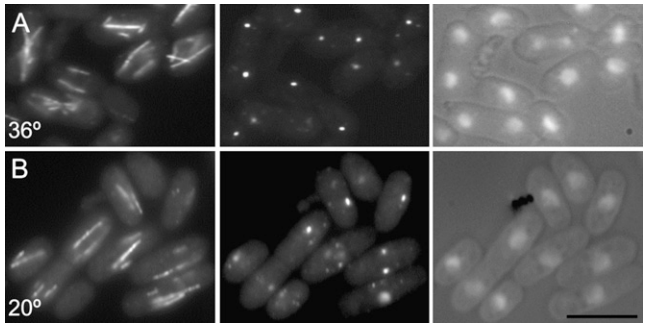

FIGURE 5.—*pla1.rt3* mutants display multiple Sad1 foci around their nuclear periphery. *pla1.rt3* cells were grown to early log phase at 36° (A) before the temperature of the medium was changed to 20° (B). Immediately before and 12 hr after the shift cells were processed for indirect immunofluorescence to reveal the distribution of microtubules (left), Sad1 protein (middle), and the relative location of the chromatin (right). Bar, 10 μm.

mutant backgrounds at either the permissive temperature of 36°, which suppresses *cut12.1* (*tfb5.rt5*), or at 20°, which is restrictive for the function of the respective Rot molecules (*rot2.1*, *pla1.rt3*) or at both (*rpl4301.rt4*, *tfb2.rt1*) (Figure 8A). Similarly, the relative levels of Cut12 were reduced below those of wild-type cells in all rot mutants at 36° and in *tfb2.rt1*, *pla1.rt3*, and *tfb5.rt5* at 20° (Figure 8B). Thus, while elevation of a mitotic inducer is sufficient to suppress Cut12, the suppression in the different *rot* mutant backgrounds does not appear to involve elevation of either Cdc25 or Cut12 levels.

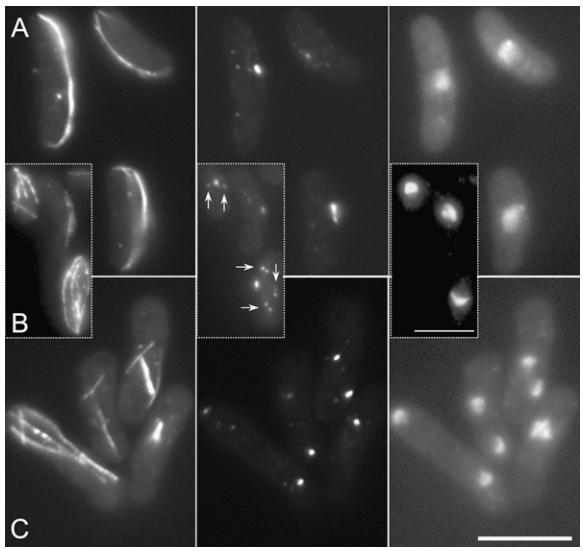

FIGURE 6.—*ded1.61* cells exhibit a "ban⁻" phenotype with multiple Sad1 foci around their nuclear periphery at 20°. (A–C) *ded1.61* cells were grown to early log phase at 36° before the temperature of the medium was changed to 20°. Fifteen hours after the shift, cells were processed for indirect immunofluorescence to reveal the distribution of microtubules (left), Sad1 protein (middle), and the relative location of the chromatin (right). Arrows highlight multiple Sad1 foci. (A and B) Interphase, (C) mitosis. Bars, 10 μm.

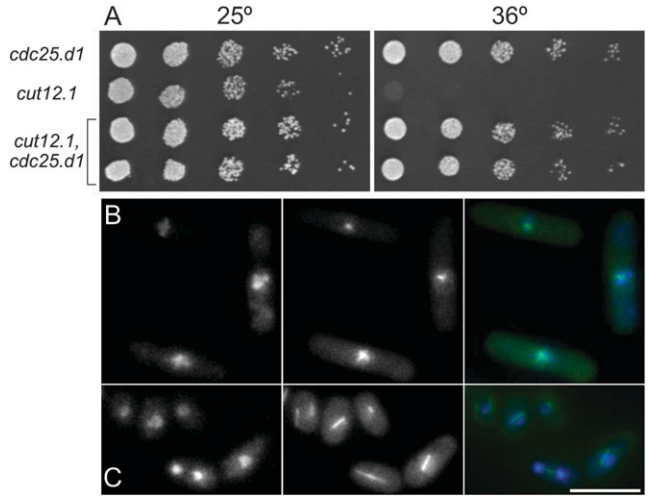

FIGURE 7.—*cdc25.d1* suppresses *cut12.1* (A) Spot tests of serial dilutions of the indicated strains on rich YES medium at the indicated temperatures. (B and C) Frames from movies of *cut12.1 atb2.gfp* and *cdc25.d1 cut12.1 atb2.gfp* cells undergoing the typical monopolar defective mitoses of *cut12.1* cells (B), or bipolar divisions of *cut12.1* cells in which the mitotic defect is compensated for by the inclusion of the *cdc25.d1* mutation. The hyperactivity conferred by the enhanced translation of the *cdc25.d1* allele accelerates mitotic commitment and so reduces cell length at commitment to mitosis (DAGA and JIMENEZ 1999).

DISCUSSION

We have used a genetic approach to identify molecules whose function can be altered to compensate for the loss of Cut12 function in the *cut12.1* mutant. To facilitate the subsequent phenotypic analyses of these mutants we selected those in which the mutation both suppressed the *cut12.1* temperature sensitivity and blocked growth at 20°. All five loci encoded molecules that are likely to influence protein levels. While it is possible that suppression arises simply from the production of more of a defective *cut12.1* protein or by readthrough of the premature stop codon in the *cut12.1* allele (BRIDGE *et al.* 1998), the monopolar spindle phenotypes arising from mutation of three of the five *rot* genes favor an intimate involvement of *rot* gene products in commitment to mitosis.

In testing the simple hypothesis that the *rot* mutants suppressed *cut12.1* because they altered the balance of mitotic inducers we found that elevation of Cdc25 levels suppressed the temperature sensitivity of *cut12.1*. Thus, not only do *cdc25.22* mutations exacerbate the spindle formation defect of *cut12.1* (BRIDGE *et al.* 1998) and hyperactivating *cut12.s11* mutations suppress deletion of *cdc25*$^{+}$ (HUDSON *et al.* 1990, 1991), but also hyperactivating mutations in *cdc25*$^{+}$ suppress loss-of-function mutations in *cut12*$^{+}$. Such reciprocal relationships strongly suggest that the spindle formation defect of *cut12.1* arises from a defect in cell-cycle control rather than an error in the nucleation of microtubules or some other physical aspect of spindle architecture.

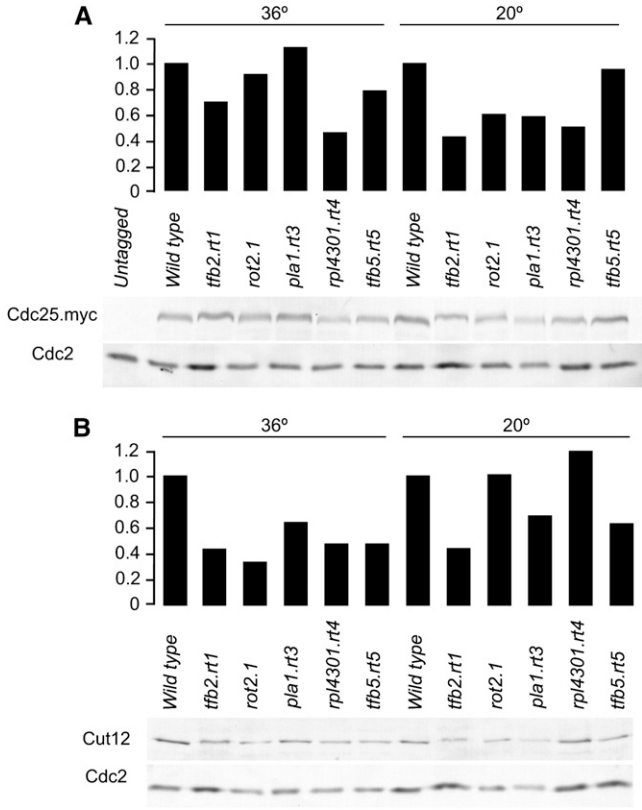

FIGURE 8.—Cdc25 and Cut12 levels decrease in *rot* mutants. Wild-type and single *rot* mutants (B) or *rot* mutants that also harbored the *cdc25.myc* allele (A) were grown to midlog phase at the permissive temperature of 36° or to early log phase and shifted to 20° for 15 hr as indicated before extracts were prepared and blotted with the 9E10 monoclonal antibody that recognized the myc epitope on Cdc25.myc or polyclonal antibodies that recognized Cut12 or Cdc2 proteins. As Cdc2 migrated lower down each respective gel the blots are from the same gels as the top panels and act as loading controls. The intensity of the bands was quantified and the Cdc25.myc and Cut12 bands were normalized to the relevant Cdc2 loading control to give the relative levels that are shown in the graphs above the blots.

This notion that a monopolar spindle phenotype can be indicative of a weak attempt at mitotic commitment would explain the impact of mutation of *wee1* upon frequency of monopolar spindles in conditional *fin1* mutants. Fin1 kinase plays a critical role in regulating mitotic commitment that is related to Cut12 and Cdc25 function. The *fin1.A5* mutation results in monopolar spindles in which only one of two SPB functions in 80% of cells at the 37° (GRALLERT and HAGAN 2002). Significantly the number of monopolar, defective, mitoses is halved by simply reducing the constraints for mitotic entry by abolishing Wee1 function (GRALLERT and HAGAN 2002). Given that genetic evidence argues that the only function of the "wee1 cdc25 switch" is to control the timing of MPF activation by modulating the phosphorylation status of tyrosine 15 of Cdc2 (FANTES 1979; RUSSELL and NURSE 1987a; GOULD and NURSE 1989), these data strongly support the notion that the *fin1* monopolar phenotype (like that of *cut12.1*) arises from defective activation of MPF during mitotic commitment.

If a monopolar spindle phenotype is indicative of a compromised commitment to mitosis, it could explain why monopolar spindles occur as a consequence of compromised TFIIH function as it was recently established that TFIIH modulates the cell-cycle levels of transcripts of mitotic inducers prior to mitosis (LEE *et al.* 2005). Compromising TFIIH activity would reduce the ability to regulate mitotic inducers to promote an efficient entrance to mitosis. Similar arguments could account for why a compromised poly(A) polymerase could reduce the ability to accumulate sufficient transcripts to get into mitosis. It is currently unclear which of the many candidate cell-cycle regulators could be altered to engender the suppression of *cut12.1* in the *rot* mutants. Cdc25 and Cut12 levels are actually reduced by mutation of *rot* mutants, making these unlikely candidates; however, it is distinctly possible that the levels of the range of inhibitory regulators including Nim1/Cdr1 or Wee1 (RUSSELL and NURSE 1987a,b; YOUNG and FANTES 1987) may be reduced or that mitotic inducers other than Cdc25 or Cut12, such as components of the stress response pathway (SHIOZAKI and RUSSELL 1995; PETERSEN and HAGAN 2005), or molecules that impinge upon the stress response pathway, may be elevated. The identification of candidate molecules requires whole proteome analyses that are beyond the scope of the current study; however, the principle established by this study that overproduction of a mitotic inducer suppresses the monopolar spindle formation phenotype of *cut12.1* extends our understanding of mitotic control.

While the intimate relationship between *cut12* and *cdc25* indicates that Cut12 is a key cell-cycle regulator, the impact of the *cut12.1* mutation upon SPB function is unilateral rather than bilateral as one becomes active while the other lies dormant or is defective. This indicates that while Cut12 can influence the global decision to commit to mitosis, it must also act at a local level to activate individual SPBs and that the two SPBs differ in their ability to respond to this second, local, function. Such disparity could arise because SPB duplication is conservative (GRALLERT *et al.* 2004) and the SPB that forms in the cell cycle after the shift to the restrictive temperature is nonfunctional. Alternatively, mitotic commitment could resemble the controls of the septum initiation network (SIN) in which the SIN is activated on the new and not the old SPB during anaphase B (SOHRMANN *et al.* 1998; GRALLERT *et al.* 2004). In this scenario only one of the two SPBs in a *cut12.1* mutant can become active because it is the only one that is mature enough to do so. In the same vein the reason that the spindle defect in Fin1 mutants is halved by abolishing Wee1 function (GRALLERT and HAGAN 2002) may also lie in a quantum difference in the response of one SPB over the other.

An interesting feature of SPB structure and function that has been revealed by the *rot* and *ded1* mutations is the proliferation of Sad1 foci. This increase in Sad1 foci is not a general feature of all SPB components in these mutants as both core SPB components Cut12 and Sid4 (Bridge *et al.* 1998; Chang and Gould 2000) remained as the single or double foci expected of SPB markers while Sad1 foci proliferated. This suggests that Sad1 plays a more peripheral role in SPB function that would be in line with the function of other members of SUN domain family proteins in higher eukaryotes where these molecules anchor centrosomes to the nuclear envelope (Tzur *et al.* 2006). A peripheral role in SPB function is also consistent with inability of excess wild-type Sad1 to alter spindle function (Hagan and Yanagida 1995). Furthermore, in the monopolar spindles of both Fin1 and Cut12 mutants Sad1 is often missing from the active SPB but accumulates on the nonfunctional SPB (Bridge *et al.* 1998; Grallert and Hagan 2002). Thus, Sad1 appears to be a peripheral SPB component that has an affinity for elements within the nuclear envelope and some level of control normally limits the amount of Sad1 incorporated into the nuclear envelope alongside the SPB. The precise nature of this control remains obscure; however, it may simply be a case of provision of the right amount of a docking protein because changes in diverse molecules that modulate transcription and translation we describe here all enhance the number of Sad1 foci on the nuclear periphery, while not causing gross alterations the levels of Sad1 itself.

While translational control and cell-cycle control have been linked at a variety of levels and it is well established that the abundance of a number of molecules oscillates as cells progress through the cell cycle, we still know relatively little about how the large number of fluctuations that have been recorded combine to determine the timing of cell-cycle transitions (Mitchison 2003). Extensive work in many systems, but principally budding yeast, have established that in all eukaryotes, signaling from the TOR pathway ensures the appropriate coupling between nutrient supply, growth, and the transition of key cell-cycle transitions (Wullschleger *et al.* 2006). In fission yeast the stress-response pathway also plays a critical role in coupling cell-cycle and differentiation decisions to nutritional status (Shiozaki and Russell 1995; Petersen and Hagan 2005). In addition a number of genetic screens designed to identify genes that would influence cell-cycle transitions in, for example, our current study, have identified mutations in molecules that modulate protein levels (Forbes *et al.* 1998; Daga and Jimenez 1999; Grallert *et al.* 2000; Liu *et al.* 2002). The frequency with which these screens and those for mitotic mutants in Drosophila (Girdham and Glover 1991; Leonard *et al.* 2003) identify DEAD box helicases highlight the critical roles that RNA processing/translational control plays in modulating cell-cycle progression (Cordin *et al.* 2005).

We thank Steve Bagley in the Paterson Institute Advanced Imaging Facility and Esther Jolley for technical assistance, Ged Brady for instruction on the customization of gene libraries, Keith Gull, Juan Jimenez, and Kayoko Tanaka for reagents, and Roger Tsien for Tdtomato fluorescent protein. Funding was supported by Cancer Research UK (CRUK).

LITERATURE CITED

Abrieu, A., T. Brassac, S. Galas, D. Fisher, J. C. Labbe *et al.*, 1998 The polo-like kinase Plx1 is a component of the MPF amplification loop at the G_2/M-phase transition of the cell cycle in Xenopus eggs. J. Cell Sci. **111:** 1751–1757.

Barbet, N., W. J. Muriel and A. M. Carr, 1992 Versatile shuttle vectors and genomic libraries for use with *Schizosaccharomyces pombe.* Gene **114:** 59–66.

Bartholomew, C. R., S. H. Woo, Y. S. Chung, C. Jones and C. F. Hardy, 2001 Cdc5 interacts with the Wee1 kinase in budding yeast. Mol. Cell. Biol. **21:** 4949–4959.

Booher, R., and D. Beach, 1988 Involvement of *cdc13*$^+$ in mitotic control in Schizosaccharomyces pombe: possible interaction of the gene-product with microtubules. EMBO J. **7:** 2321–2327.

Bridge, A. J., M. Morphew, R. Bartlett and I. M. Hagan, 1998 The fission yeast SPB component Cut12 links bipolar spindle formation to mitotic control. Genes Dev. **12:** 927–942.

Chang, L., and K. L. Gould, 2000 Sid4p is required to localize components of the septum intiation pathway to the spindle pole body in fission yeast. Proc. Natl. Acad. Sci. USA **97:** 5249–5254.

Cordin, O., J. Banroques, N. K. Tanner and P. Linder, 2005 The DEAD-box protein family of RNA helicases. Gene **367:** 17–37.

Creanor, J., and J. M. Mitchison, 1994 The kinetics of H1 kinase activation during the cell cycle of wild type and *wee* mutants of the fission yeast *Schizosaccharomyces pombe.* J. Cell Sci. **107:** 1197–1204.

Daga, R. R., and J. Jimenez, 1999 Translational control of the Cdc25 cell cycle phosphatase: a molecular mechanism coupling mitosis to cell growth. J. Cell Sci. **112:** 3137–3146.

Ding, D.-Q., Y. Tomita, A. Yamamoto, Y. Chikashige, T. Haraguchi *et al.*, 2000 Large-scale screening of intracellular protein localization in living fission yeast by the use of GFP-fusion genomic DNA library. Genes Cells **5:** 169–190.

Evan, G. I., G. K. Lewis, G. Ramsay and J. M. Bishop, 1985 Isolation of monoclonal-antibodies specific for human c-myc proto-oncogene product. Mol. Cell. Biol. **5:** 3610–3616.

Evans, T., E. T. Rosenthal, J. Youngblom, D. Distel and T. Hunt, 1983 Cyclin: a protein specified by maternal mRNA in sea urchin eggs that is destroyed at each cleavage division. Cell **33:** 389–396.

Fantes, P., 1979 Epistatic gene interactions in the control of division in fission yeast. Nature **279:** 428–430.

Fantes, P. A., 1983 Control of timing of cell-cycle events in fission yeast by the *wee1*$^+$ gene. Nature **302:** 153–155.

Featherstone, C., and P. Russell, 1991 Fission yeast p107wee1 mitotic inhibitor is a tyrosine/serine kinase. Nature **349:** 808–811.

Fisher, D. L., and P. Nurse, 1996 A single fission yeast mitotic cyclin-B p34^{Cdc2} kinase promotes both S-Phase and mitosis in the absence of G_1 cyclins. EMBO J. **15:** 850–860.

Forbes, K. C., T. Humphrey and T. Enoch, 1998 Suppressors of cdc25p overexpression identify two pathways that influence the G2/M checkpoint in fission yeast. Genetics **150:** 1361–1375.

Girdham, C. H., and D. M. Glover, 1991 Chromosome tangling and breakage at anaphase result from mutations in Lodestar, a Drosophila gene encoding a putative nucleoside triphosphate-binding protein. Genes Dev. **5:** 1786–1799.

Gould, K. L., and P. Nurse, 1989 Tyrosine phosphorylation of the fission yeast Cdc2+ protein-kinase regulates entry into mitosis. Nature **342:** 39–45.

Grallert, A., and I. M. Hagan, 2002 *Schizosaccharomyces pombe* NIMA-related kinase Fin1 regulates spindle formation and an affinity of Polo for the SPB. EMBO J. **21:** 3096–3107.

Grallert, A., A. Krapp, S. Bagley, V. Simanis and I. M. Hagan, 2004 Recruitment of NIMA kinase shows that maturation of the *S. pombe* spindle-pole body occurs over consecutive cell cycles and reveals a role for NIMA in modulating SIN activity. Genes Dev. **18:** 1007–1021.

Grallert, B., S. E. Kearsey, M. Lenhard, C. R. Carlson, P. Nurse *et al.*, 2000 A fission yeast general translation factor reveals links between protein synthesis and cell cycle controls. J. Cell. Sci. **113**(8): 1447–1458.

Hagan, I., and M. Yanagida, 1995 The product of the spindle formation gene *sad1*$^+$ associates with the fission yeast spindle pole body and is essential for viability. J. Cell Biol. **129:** 1033–1047.

Hirano, T., S. Funahashi, T. Uemura and M. Yanagida, 1986 Isolation and characterization of *Schizosaccharomyces pombe* cut mutants that block nuclear division but not cytokinesis. EMBO J. **5:** 2973–2979.

Hoffmann, I., P. R. Clarke, M. J. Marcote, E. Karsenti and G. Draetta, 1993 Phosphorylation and activation of human cdc25-C by cdc2-cyclin B and its involvement in the self amplification of MPF at mitosis. EMBO J. **12:** 53–60.

Hudson, J. D., H. Feilotter and P. G. Young, 1990 *stf1*: non-wee mutations epistatic to *cdc25* in the fission yeast *Schizosaccharomyces pombe*. Genetics **126:** 309–315.

Hudson, J. D., H. Feilotter, C. Lingner, R. Rowley and P. Young, 1991 *stf1*: a new supressor of the mitotic control gene *cdc25* in *Schizosaccharomyces pombe*. Cold Spring Harbor Symp. Quant. Biol. **56:** 599–604.

Izumi, T., and J. L. Maller, 1993 Elimination of cdc2 phosphorylation sites in the cdc25 phosphatase blocks initiation of M-phase. Mol. Biol. Cell **4:** 1337–1350.

Izumi, T., and J. Maller, 1995 Phosphorylation and activation of *Xenopus* Cdc25 phosphatase in the absence of Cdc2 and Cdk2 kinase activity. Mol. Biol. Cell **6:** 215–226.

Jackman, M., C. Lindon, E. A. Nigg and J. Pines, 2003 Active cyclin B1-Cdk1 first appears on centrosomes in prophase. Nat. Cell Biol. **5:** 143–148.

Karaiskou, A., C. Jessus, T. Brassac and R. Ozon, 1999 Phosphatase 2A and Polo kinase, two antagonistic regulators of Cdc25 activation and MPF auto-amplification. J. Cell Sci. **112:** 3747–3756.

Karaiskou, A., A. C. Lepretre, G. Pahlavan, D. Du Pasquier, R. Ozon *et al.*, 2004 Polo-like kinase confers MPF autoamplification competence to growing Xenopus oocytes. Development **131:** 1543–1552.

Keeney, J. B., and J. D. Boeke, 1994 Efficient targeted integration at leu1-32 and ura4-294 in *Schizosaccharomyces pombe*. Genetics **136:** 849–856.

Kovelman, R., and P. Russell, 1996 Stockpiling of Cdc25 during a DNA-replication checkpoint arrest in *Schizosaccharomyces pombe*. Mol. Cell. Biol. **16:** 86–93.

Kumagai, A., and W. G. Dunphy, 1996 Purification and molecular-cloning of Plx1, a Cdc25-regulatory kinase from Xenopus egg extracts. Science **273:** 1377–1380.

Lane, H. A., and E. A. Nigg, 1996 Antibody microinjection reveals an essential role for human polo-like kinase 1 (Plk1) in the functional maturation of mitotic centrosomes. J. Cell Biol. **135:** 1701–1713.

Lee, K. M., I. Miklos, H. Du, S. Watt, Z. Szilagyi *et al.*, 2005 Impairment of the TFIIH-associated CDK-activating kinase selectively affects cell cycle-regulated gene expression in fission yeast. Mol. Biol. Cell **16:** 2734–2745.

Leonard, D., P. Ajuh, A. L. Lamond and R. J. Legerski, 2003 hLodestar/HuF2 interacts with CDC5L and is involved in pre-mRNA splicing. Biochem. Biophys. Res. Commun. **308:** 793–801.

Liu, H. Y., B. S. Nefsky and N. C. Walworth, 2002 The Ded1 DEAD box helicase interacts with Chk1 and Cdc2. J. Biol. Chem. **277:** 2637–2643.

Lopez-Girona, A., B. Furani, O. Mondesert and P. Russell, 1999 Nuclear localisation of Cdc25 is regulated by DNA damage and a 14–3-3 protein. Nature **397:** 172–175

MacIver, F. H., K. Tanaka, A. M. Robertson and I. M. Hagan, 2003 Physical and functional interactions between polo kinase and the spindle pole component Cut12 regulate mitotic commitment in *S. pombe*. Genes Dev. **17:** 1507–1523.

McGowan, C. H., and P. Russell, 1993 Human Wee1 kinase inhibits cell division by phosphorylating p34^{cdc2} exclusively on Tyr15. EMBO J. **12:** 75–85.

Mitchison, J. M., 2003 Growth during the cell cycle. Int. Rev. Cytol. **226:** 165–258.

Moreno, S., A. Klar and P. Nurse, 1991 Molecular genetic analysis of fission yeast *Schizosaccharomyces pombe*. Methods Enzymol. **194:** 795–823.

Mueller, P. R., T. R. Coleman and W. G. Dunphy, 1995 Cell-cycle regulation of a Xenopus Wee1-like kinase. Mol. Biol. Cell **6:** 119–134.

Mulvihill, D. P., J. Petersen, H. Ohkura, D. M. Glover and I. M. Hagan, 1999 Plo1 kinase recruitment to the spindle pole body and its role in cell division in *Schizosaccharomyces pombe*. Mol. Biol. Cell **10:** 2771–2785.

Nurse, P., 1990 Universal control mechanism regulating onset of M-phase. Nature **344:** 503–508.

Ohnacker, M., L. Minvielle-Sebastia and W. Keller, 1996 The Schizosaccharomyces pombe *pla1* gene encodes a poly(A) polymerase and can functionally replace its *Saccharomyces cerevisiae* homologue. Nucleic Acids Res. **24:** 2585–2591.

Parker, L. L., and H. Piwnicaworms, 1992 Inactivation of the p34^{cdc2}cyclinB complex by the human Wee1 tyrosine kinase. Science **257:** 1955–1957.

Petersen, J., and I. M. Hagan, 2005 Polo kinase links the stress pathway to cell cycle control and tip growth in fission yeast. Nature **435:** 507–512.

Russell, P., and P. Nurse, 1986 *Cdc25*$^+$ functions as an inducer in the mitotic control of fission yeast. Cell **45:** 145–153.

Russell, P., and P. Nurse, 1987a Negative regulation of mitosis by *wee1*$^+$, a gene encoding a protein- kinase homolog. Cell **49:** 559–567.

Russell, P., and P. Nurse, 1987b The mitotic inducer *nim1*$^+$ functions in a regulatory network of protein-kinase homologs controlling the initiation of mitosis. Cell **49:** 569–576.

Sakchaisri, K., S. Asano, L. R. Yu, M. J. Shulewitz, C. J. Park *et al.*, 2004 Coupling morphogenesis to mitotic entry. Proc. Natl. Acad. Sci. USA **101:** 4124–4129.

Shiozaki, K., and P. Russell, 1995 Cell-cycle control linked to extracellular environment by MAP kinase pathway in fission yeast. Nature **378:** 739–743.

Simanis, V., and P. Nurse, 1986 The cell-cycle control gene cdc2$^+$ of fission yeast encodes a protein-kinase potentially regulated by phosphorylation. Cell **45:** 261–268.

Sohrmann, M., S. Schmidt, I. Hagan and V. Simanis, 1998 Asymmetric segregation on spindle poles of the *Schizosaccharomyces pombe* septum-inducing protein kinase Cdc7p. Genes Dev. **12:** 84–94.

Stevenson, A. L., and C. J. Norbury, 2006 The Cid1 family of non-canonical poly(A) polymerases. Yeast **23:** 991–1000.

Tang, Z. H., T. R. Coleman and W. G. Dunphy, 1993 Two distinct mechanisms for negative regulation of the wee1 protein- kinase. EMBO J. **12:** 3427–3436.

Tzur, Y. B., K. L. Wilson and Y. Gruenbaum, 2006 SUN-domain proteins: 'Velcro' that links the nucleoskeleton to the cytoskeleton. Nat. Rev. Mol. Cell Biol. **7:** 782–788.

Verde, F., J. Mata and P. Nurse, 1995 Fission yeast-cell morphogenesis: identification of new genes and analysis of their role during the cell-cycle. J. Cell Biol. **131:** 1529–1538.

Watanabe, N., H. Arai, Y. Nishihara, M. Taniguchi, N. Watanabe *et al.*, 2004 M-phase kinases induce phospho-dependent ubiquintination of somatic Wee1 by SCFβ-TrCP. Proc. Natl. Acad. Sci. USA **101:** 4419–4424.

Woods, A., T. Sherwin, R. Sasse, T. H. Macrae, A. J. Baines *et al.*, 1989 Definition of individual components within the cytoskeleton of *Trypanosoma brucei* by a library of monoclonal-antibodies. J. Cell Sci. **93:** 491–500.

Wullschleger, S., R. Loewith and M. N. Hall, 2006 TOR signalling in growth and metabolism. Cell **124:** 471–484.

Young, P. G., and P. A. Fantes, 1987 *Schizosaccharomyces pombe* mutants affected in their division response to starvation. J. Cell Sci. **88:** 295–304.

Yu, J., Y. Zhao, Z. Li, S. Galas and M. L. Goldberg, 2006 Greatwall kinase participates in the CDC2 autoregulatory loop in Xenopus egg extracts. Mol. Cell **22:** 83–91.

Communicating editor: P. Russell